AIAA JOURNAL
Vol. 32, No. 1, January 1994

Treatment of Material Creep and Nonlinearities in Flexible Multibody Dynamics

M. Xie* and F. M. L. Amirouche†
University of Illinois at Chicago, Chicago, Illinois 60680

This paper addresses the modeling of the generalized active forces resulting from deformable bodies when subjected to high temperature conditions, elastic-plastic deformations, creep effects, and material nonlinearities. The effects of elastic-plastic deformations are studied making use of the nonlinear stress-strain relationship and the geometrical stiffness concepts. Creep conditions resulting from high temperature are studied through several proposed models. Material nonlinearities for isotropic and composites are accounted for by their tangential elasticity matrix. A general procedure used in the study of multibody systems dynamics with elastic-plastic bodies depicting the characteristics mentioned is developed. This includes an explicit formulation of the equations of motion using Kane's equations, finite element method, continuum mechanics, and modal coordinate reduction techniques. A numerical simulation of a flexible robotic arm with a prescribed angular velocity subject to high temperature conditions is analyzed. The effects of creep are discussed.

I. Introduction

THE analysis and prediction of the dynamic behavior of complex mechanical systems has become an important part of modern engineering. For the past two decades multibody dynamics researchers and scientists have developed methodologies, computational algorithms, and general purpose codes capable of simulating a large class of applications. Although some of the problems in multibody dynamics have been resolved, others still remain to be issues of concern. The modeling of nonlinearities and deformations are subjects that need further studying. For example, it was demonstrated by Kane et al.[6] among others[1] that geometric stiffening effects in beams play a crucial role in high-speed spin-up motion. Formulations to account for such nonlinearities can be done in two ways. One is through the constraint relationship between elastic displacements and the other is to introduce these effects through the nonlinear strain energy function.[2,6] Similarly, one can introduce the effects of temperature on the body deformation making use of the relationship between the strain and temperature.[9,20,21,22,23,28]

The effects of large deformation is the subject of this paper. It was shown by a number of researchers[10–14] that a finite element method can be used successfully in the context of Lagrange dynamics to account for large strains. Those methods were used in particular in the study of crash simulations. This paper combines the concepts of continuum mechanics in relating the nonlinear strain deformations to the body and external forces and applies a finite element together with Kane's equation in dynamics to formulate a set of differential equations to describe the dynamics of deformable bodies undergoing large rotations and displacements.

The paper first addresses the force displacement relationship for both small and large deformation and finally gives the corresponding general form of the generalized active forces. The governing equations of motion are derived using a matrix form presented by Amirouche and Xie in Ref. 7 and by Amirouche in Ref. 8. Finally, numerical simulations considering the effect of creep under high temperature conditions are presented.

Received June 29, 1992; revision received May 20, 1993; accepted for publication May 22, 1993.

*Ph.D. Research Assistant, Department of Mechanical Engineering.
†Professor, Department of Mechanical Engineering. Member AIAA

II. Generalized Active Force Formulation

A. Effects of Creep and Temperature

The constitutive law of creep can be a form in which the rate of creep strain is defined as some function of stresses and total creep strain, that is,

$$\dot{\epsilon}_c = \frac{d\epsilon_c}{dt} = \beta(\sigma, \epsilon_c) \tag{1}$$

Andrade[15] found that the creep curve could be represented by the following empirical equation:

$$\epsilon_c = \epsilon_0\left(1 + \beta t^{1/3}\right)e^{\kappa t} \tag{2}$$

where β and κ are constants. The transient creep is represented by β and Eq. (2) refers to this form when $\kappa = 0$. The constant κ describes an extension per unit length which proceeds at a constant rate. Garofalo[16] gives an equation with better fit than Andrade's equation, although it has been tested on a limited number of materials

$$= \epsilon_0 + \epsilon_t(1 - e^{-rt}) + \dot{\epsilon}_s t \tag{3}$$

where ϵ_0 is the instantaneous strain on loading, ϵ_t the limit for transient creep, r the ratio of transient creep rate to the transient creep strain, and $\dot{\epsilon}_s$ the steady-state creep rate.

The so-called Bailey-Norton law gives the following equation for creep strain[17]:

$$\epsilon_c = A\sigma^m t^n \tag{4}$$

where A, m, and n are constants that are functions of temperature. From Eq. (4) we can get the so-called time-hardening formulation for the creep strain[17]:

$$\dot{\epsilon}_c = \frac{\partial \epsilon_c}{\partial t} = A\sigma^m n t^{n-1} \tag{5}$$

or the strain-hardening formulation

$$\dot{\epsilon}_c = A^{1/n} n \sigma^{m/n} \epsilon_c^{1-(1/n)} \tag{6}$$

The preceding equations constitute only a partial summary of creep strain equations.

The total strains of a deformable body subject to creep, temperature, and elastic-plastic deformations can be defined as

$$\epsilon = \epsilon_e + \epsilon_c + \epsilon_p + \alpha T \tag{7}$$

where ϵ_e is the elastic strain, ϵ_p the plastic strain which is discussed in the next section, α the linear coefficient of thermal expansion, and T the temperature. From Eq. (7) the elastic strain can be expressed as

$$\epsilon_e = \epsilon - \epsilon_c - \alpha T \tag{8}$$

where ϵ_p has been omitted for now and will be dealt with in the next section. Consider a discretized body. Using the finite element method procedures, we can write the force-strain relationship as

$$\{f\} = \int_v [B]^T [D] [B] \, dv \{p\} - \int_v [B]^T [D] (\{\epsilon_c\} + \alpha \{T\}) \tag{9}$$

i.e.,

$$\{f\} = [K] \{p\} - \{f_T\} \tag{10}$$

where

$$[K] = \int_v [B]^T [D] [B] \, dv \tag{11}$$

is the ordinary stiffness matrix, $[B]$ and $[D]$ define the strain shape function and material property matrices, respectively, and

$$\{f_T\} = \int_v [B]^T [D] (\{\epsilon_c\} + \alpha \{T\}) \, dv \tag{12}$$

is the equivalent force due to creep and temperature. In multibody dynamic systems the creep condition could be regarded as a dynamic creep. Hence, we can get the alternative stress σ, as depicted by Eq. (4), or simply the instantaneous strain ϵ_0, defined by Eq. (2) and (3), by premultiplying the strain of the steady-state creep by a coefficient k, $0.5 < k < 1$, which is usually found by experiment.

Note that if the temperature T is a function of the space coordinates, say,

$$T = T(\rho) = T[\rho(x, y, z)] \tag{13}$$

then we should add one more term to the equivalent body force to account for the rate of temperature change

$$\{f_T^b\} - \int [N]^T [D] \alpha \{T'\} \, dv \tag{14}$$

where

$$\{T'\} = \left[\frac{\partial T}{\partial x} \frac{\partial T}{\partial y} \frac{\partial T}{\partial z}\right]^T$$

When the thermal stress is generated through sudden changes in temperature, the process is referred to as thermal shock. For instance, robots handling metal heat treatments are part of these engineering applications. Although thermal shock stresses are determined by the temperature distribution, the steady-state condition might result in different values. Such stresses are often greater than those due to slow heating and cooling, because of the steep temperature gradients that can be generated. A distinction between ordinary thermal stress and thermal shock stress is the initial high stress application observed in thermal shock. Many materials are affected by the rate at which load is applied. The strain caused by thermal shock is given by Manson[22]

$$\epsilon_T = \sigma^* \alpha T_0 \tag{15}$$

where ϵ_T is strain due to thermal shock; and $\sigma^* = (T_{av} - T)/T_0$, where T_{av} denotes the average temperature of the body undergoing thermal shock, T temperature at the point where stress is considered, and T_0 initial uniform temperature of the body above the ambient temperature which can be assumed zero for simplicity. The stress σ^* can be obtained from experiment. Thus we can add the strain due to the effects of temperature ϵ_T to Eq. (8), and the influence of thermal shock is then considered.

B. Effects of Elastic-Plastic Deformation

Plastic behavior of materials is characterized by a nonunique stress-strain relationship. The definition of plasticity may be the presence of unrecoverable strains on load removal.

Uniaxial behavior of materials can be of four types: nonlinear elastic-plastic, perfect plastic, and strain-hardening plasticity. It is quite generally postulated, as an experimental fact, that yielding can occur only if the stress σ satisfies the general yield criterion

$$F(\sigma, \kappa) = 0 \tag{16}$$

where κ is a hardening parameter. This yield condition can be visualized as a surface in n-dimensional space of stress with the position of the surface dependent on the instantaneous value of the parameter κ. Assume that the strain increment can be decomposed into the sum of a plastic part and of an elastic part, thus,

$$\{d\epsilon\} = \{d\epsilon_e\} + \{d\epsilon_p\} \tag{17}$$

where

$$\{d\epsilon_p\} = \lambda \left\{\frac{\partial F}{\partial \sigma}\right\} \tag{18}$$

For simplicity the associated plasticity in yield criterion is assumed; otherwise, the function F is replaced with $Q = Q(\sigma, \kappa)$ which denotes the plastic potential, and λ is an undetermined proportionality constant. Since

$$\{\sigma\} = [D] \{\epsilon_e\} \tag{19}$$

where $[D]$ denotes the ordinary material property matrix, and

$$dF = \sum_i \frac{\partial F}{\partial \sigma_i} d\sigma_i + \frac{\partial F}{\partial \kappa} d\kappa = \left\{\frac{\partial F}{\partial \sigma}\right\}^T \{d\sigma\} + \frac{\partial F}{\partial \kappa} d\kappa = 0 \tag{20}$$

where

$$dK = \sum_i \sigma_i d\epsilon_i^p = \{\sigma\}^T \{d\epsilon_p\} \tag{21}$$

Making use of Eqs. (20) and (21), we can write

$$\left\{\frac{\partial F}{\partial \sigma}\right\}^T \{d\sigma\} = -\frac{\partial F}{\partial \kappa} \{\sigma\}^T \{d\epsilon_p\} = -\lambda \frac{\partial F}{\partial \kappa} \{\sigma\}^T \left\{\frac{\partial F}{\partial \sigma}\right\} \tag{22}$$

Let

$$A = -\frac{\partial F}{\partial \kappa} d\kappa \frac{1}{\lambda}$$

Then Eq. (22) becomes

$$\left\{\frac{\partial F}{\partial \sigma}\right\}^T \{d\sigma\} - A\lambda = 0 \tag{23}$$

Making use of Eqs. (16–19) we get

$$\{d\epsilon\} = [D]^{-1}\{d\sigma\} + \lambda\left\{\frac{\partial F}{\partial \sigma}\right\} \tag{24}$$

Multiplying by $\{\partial F/\partial\sigma\}^T[D]$ yields

$$\left\{\frac{\partial F}{\partial \sigma}\right\}^T\{d\sigma\} = \left\{\frac{\partial F}{\partial \sigma}\right\}^T[D]\{d\epsilon\} - \left\{\frac{\partial F}{\partial \sigma}\right\}^T[D]\left\{\frac{\partial F}{\partial \sigma}\right\}\lambda \tag{25}$$

Substituting the preceding equations into Eq. (23) we arrive at

$$\left\{\frac{\partial F}{\partial \sigma}\right\}^T[D]\{d\epsilon\} - \left(\left\{\frac{\partial F}{\partial \sigma}\right\}^T[D]\left\{\frac{\partial F}{\partial \sigma}\right\} + A\right)\lambda = 0 \tag{26}$$

Elimination of λ from Eqs. (25) and (26) gives

$$[D_{ep}] = [D] - [D]\left\{\frac{\partial F}{\partial \sigma}\right\}\left\{\frac{\partial F}{\partial \sigma}\right\}^T[D]\left(A + \left\{\frac{\partial F}{\partial \sigma}\right\}^T[D]\left\{\frac{\partial F}{\partial \sigma}\right\}\right)^{-1} \tag{27}$$

The stress-relationship can be expressed as

$$\{d\sigma\} = [D_{ep}]\{d\epsilon\} \tag{28}$$

where $[D_{ep}]$ is the elasto-plasticity matrix replacing the elasticity matrix $[D]$ in incremental analysis. If the well-known Huber-von Mises yield surface is assumed, then the yield criterion can be obtained from Chen and Han[19] as

$$\begin{aligned} F &= [{}^1/_2(\sigma_1-\sigma_2)^2 + {}^1/_2(\sigma_2-\sigma_3)^2 + {}^1/_2(\sigma_3-\sigma_1)^2 \\ &\quad + 3\sigma_{12}^2 + 3\sigma_{23}^2 + 3\sigma_{31}^2]^{1/2} - \sigma_y \\ &\equiv \bar{\sigma} - \sigma_y \end{aligned} \tag{29}$$

where $\sigma_y = \sigma_y(\kappa)$ is the uniaxial stress at yield.

Let s_i $(i = 1, 2, 3)$ represent the deviatoric stresses, i.e.,

$$s_i = \sigma_i - \frac{1}{3}\sum_{i=1}^{3}\sigma_i \tag{30}$$

then

$$\frac{\partial F}{\partial \sigma_{ij}} = \begin{cases} \dfrac{3s_i}{2\bar{\sigma}} & \text{for} \quad i = 1,2,3 \quad \text{and} \quad i = j \\ \dfrac{3\sigma_{ij}}{\bar{\sigma}} & \text{otherwise} \end{cases} \tag{31}$$

If a plot of the uniaxial test giving $\bar{\sigma}$ vs the plastic uniaxial strain ϵ_{up} is available and if simple work hardening is assumed, we can evaluate the coefficient A from Eq. (23). [The slope of the stress $\bar{\sigma}$ given by Eq. (29) defines such a value.]

On the other hand, if another yield theory is assumed, say, Tresca, as denoted by Chen and Han,[19] then

$$F = 2\bar{\sigma}\cos\theta - Y(\kappa) = 0 \tag{32}$$

where $Y(\kappa)$ denotes the yield stress from uniaxial tests, and

$$\theta = 1/3\sin^{-1}\left(-\frac{3\sqrt{3}J_3}{2\bar{\sigma}^3}\right) \qquad -\frac{\pi}{6} < \theta < \frac{\pi}{6} \tag{33}$$

where

$$J_3 = s_1s_2s_3 + 2\sigma_{12}\sigma_{23}\sigma_{31} - s_1\sigma_{23}^2 - s_2\sigma_{31}^2 - s_3\sigma_{12}^2 \tag{34}$$

Actually, we can write $[D_{ep}]$ as a sum of two matrices

$$[D_{ep}] = [D] + [D_p] \tag{35}$$

where $[D]$ denotes the ordinary material property matrix, and $[D_p]$ represents the material plasticity property matrix.

C. Effects of Material and Geometric Nonlinearities

The ordinary stiffness matrices are based on small deformation and material linearity. In this case the solution can be obtained by deleting quadratic terms in the strain-displacement relations. But when the deformation is large enough to cause significant change in the geometry of the deformed body, we have to consider the nonlinearity between strain and displacement, that is, geometric elastic nonlinearity. Similarly, many problems of practical consequence can exist in which such material linear elasticity is not presented, i.e., we cannot find the Young's modulus to make the formula $\sigma = E\epsilon$ hold.

Case 1: Isotropic Material

Let us assume the nonlinear elastic behavior of a body which can be governed by the following stress function:

$$\sigma = \sigma(\varepsilon) \tag{36}$$

then the so-called tangential stiffness matrix is given by

$$\begin{aligned} [K_t] &= \int_v [B]^T\left[\frac{d\sigma}{d\rho}\right]dv = \int_v [B]^T\left[\frac{d\sigma}{d\epsilon}\right]\left[\frac{d\epsilon}{d\rho}\right]dv \\ &= \int_v [B]^T[D_t][B]\,dv \end{aligned} \tag{37}$$

where ρ is the nodal coordinate and

$$[D_t] = \left[\frac{d\sigma}{d\epsilon}\right] \tag{38}$$

is known as the tangential elasticity matrix.

Sometimes departures from linearity occur only at higher values of stress or strain; then it is convenient to compare the relationship given by Eq. (36) with the linear one given by

$$\{\sigma\} = [D](\{\epsilon\} - \{\epsilon_0\}) + \{\sigma_0\} \tag{39}$$

where ϵ_0 denotes the initial strain due to temperature changes, shrinkage, crystal growth, and so on and σ_0 is the initial residual stress. Clearly, it is possible to make this equivalent to the general statement given by Eq. (36) by expressing ϵ_0 or σ_0 as functions of the strain level, where these functions have zero values at small strain levels.

Case 2: Composites

Composite material are widely used in aerospace and automotive engineering. Many military and civil aircrafts contain substan-

tial quantities of lightweight, high-strength carbon Keolar and glass fiber composites, as laminated panels and moldings, and as composite honeycomb structures with metallic or resin-impregnated paper honeycomb core materials. For elevated temperature applications carbon-fiber-reinforced-carbon is in use or is under consideration. Rocket motor casings and rocket launchers are also frequently made of reinforced plastics. Again, there is an increasing interest in weight reduction to achieve energy conservation and motoring economy.

In a general three-dimensional orthotropic case, the material property matrix is given by

$$[D] = [\mathcal{C}]^{-1} \tag{40}$$

where $[\mathcal{C}]$ represents the material compliance matrix and is expressed as

$$[\mathcal{C}] = \begin{bmatrix} \frac{1}{E_1} & -\frac{\nu_{12}}{E_1} & -\frac{\nu_{13}}{E_1} & 0 & 0 & 0 \\ -\frac{\nu_{21}}{E_2} & \frac{1}{E_2} & -\frac{\nu_{23}}{E_2} & 0 & 0 & 0 \\ -\frac{\nu_{31}}{E_3} & -\frac{\nu_{32}}{E_3} & \frac{1}{E_3} & 0 & 0 & 0 \\ 0 & 0 & 0 & \frac{1}{G_{12}} & 0 & 0 \\ 0 & 0 & 0 & 0 & \frac{1}{G_{23}} & 0 \\ 0 & 0 & 0 & 0 & 0 & \frac{1}{G_{31}} \end{bmatrix} \tag{41}$$

with

$$\nu_{12}E_2 = \nu_{21}E_1 \qquad \nu_{13}E_3 = \nu_{31}E_1 \qquad \nu_{23}E_3 = \nu_{32}E_2$$

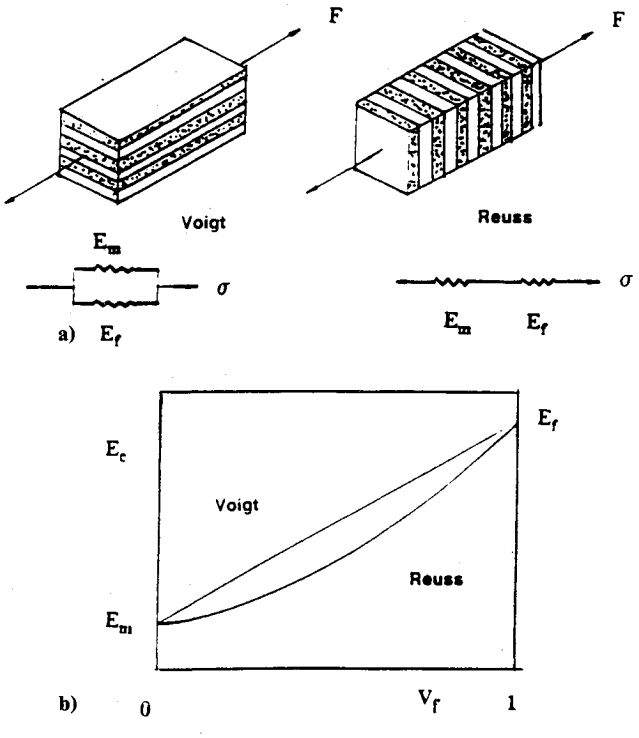

Fig. 1 Composites and their models.

where E_i and ν_{ij} $(i, j = 1, 2, 3)$ are Young's moduli and Poisson ratios of materials, respectively.

References 24–27 give the methods used in computing the Young's moduli and Poisson ratios. For example, the simplest approach to calculate the elastic response of composites is to imagine, in extreme cases, arrays of well-bonded lamellae having different moduli but identical Poisson ratios, as shown in Fig. 1a. For case a, there is continuity of strain at the interfaces, and we can consider the model as a parallel arrangement of springs. For case b, it is considered as a series arrangement of springs since there is continuity of stress. Simple arithmetic gives the longitudinal elastic modulus for each model, and the parallel and series estimates are the Voigt and Reuss estimates shown in Fig. 1b.

Voigt

$$E_c = E_m V_m + E_f V_f \tag{42}$$

Reuss

$$\frac{1}{E_c} = \frac{V_f}{E_f} + \frac{V_m}{E_m} \tag{43}$$

where the subscripts c, m, and f are the composite, fiber, and matrix material, respectively. V_f and V_m denote the volumes of fiber and matrix material, with $V_m + V_f = 1$.

For the transverse modulus of fiber composites, a simple approach is to use an empirical "contiguity" factor c, such that

$$E_t = E_{\text{Reuss}} + c\,(E_{\text{Voigt}} - E_{\text{Reuss}}) \tag{44}$$

which was introduced by Tsai in 1964.[27]

If the laminates are assumed to consist of perfectly bounded laminae where bonds are assumed to be infinitesimally thin as well as nonshear deformable, then the effective material property matrix of the overall laminate of element i of body j is given by

$$[D^{ji}] = \sum_{k=1}^{n} \frac{t_k^{ji}}{h^{ji}} [D_k^{ji}] \tag{45}$$

where n denotes the number of laminae, t_k^{ji} the thickness of the kth lamina in a laminate of thickness h^{ji}, and $[D_k^{ji}]$ the material property matrix of a lamina k with respect to the laminate coordinate system, and

$$[D_k^{ji}] = [S^{ji}]\,[\bar{D}_k^{ji}]\,[S^{ji}]^T \tag{46}$$

where $[S^{ji}]$ denotes the transformation matrix from the coordinate system of element i to that of body j and $[\bar{D}_k^{ji}]$ the material property matrix defined in the coordinate system of element i.

Case 3: Geometric Nonlinearities

To solve the geometric nonlinearity problem arising from large deformations, we can write the strain shape function matrix as

$$[B_G] = [B] + [B_L(\rho)] \tag{47}$$

where $[B_G]$ is defined from the strain definition as

$$\{d\epsilon\} = [B_G]\,\{d\rho\} \tag{48}$$

$[B]$ is the same matrix as that in the linear infinitesimal strain analysis, and only $[B_L]$ depends on the displacement. In general, $[B_L]$ will be found to be a linear function of such displacements. Then the total tangential stiffness matrix $[K_T]$ (needed in the finite element method to relate the force displacement) will be expressed as

$$[K_T] = [K] + [K_G] \tag{49}$$

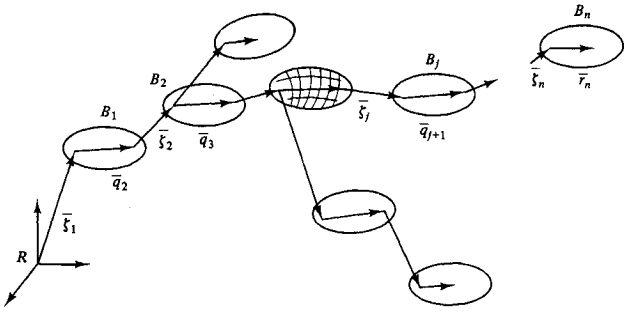

Fig. 2 Treelike multibody system.

where $[K]$ is the ordinary stiffness matrix and

$$[K_G] = [K_L] + [K_\sigma] \tag{50}$$

$[K_L]$ is the contribution of large displacement and is given by

$$[K_L] = \int_v ([B]^T[D][B_L] + [B_L]^T[D][B_L] + [B_L]^T[D][B_L]) \, dv \tag{51}$$

which is called the initial displacement matrix or large displacement matrix; and $[K_\sigma]$ is known as the initial stress matrix.

Ider and Amirouche in Ref. 29 gave the explicit form of geometric nonlinearities for three-dimensional and two-dimensional beams using the strain energy method.

III. Governing Equations of Motion

For the flexible treelike multibody system shown in Fig. 2, let each body be assumed flexible. Furthermore, let each body be discretized into n elements. Then employing the recursive method, we derive the equations of motion. The latter is accomplished by defining the position vector from fixed inertial frame $\boldsymbol{R}$ starting at its center O and making use of intermediate body vectors q and ζ (as shown in Fig. 2). The differentiation of the position vector yields the element mass center velocity in $\boldsymbol{R}$. In a similar fashion we obtain the mass center acceleration. We integrate over the volume of the element to formulate the element inertia forces and moments. From procedures and strategic partitioning and definition of the generalized speeds outlined by Amirouche in Ref. 8, the equations of motion take the following form:

$$[M]\{\ddot{y}\} + C\{\dot{y}\} + [K]\{y\} = \{F\} \tag{52}$$

where $\{y\} = \{x^T \zeta^T \rho^T\}^T$; x and ζ denote the relative body rotations expressed in terms of Euler angles and the relative body translations, respectively; whereas ρ denotes the nodal coordinates of the elements. The generalized mass matrix $[M]$ is found to be

$$[M] = \begin{bmatrix} M_{11} & M_{12} & M_{13} \\ M_{21} & M_{22} & M_{23} \\ M_{31} & M_{32} & M_{33} \end{bmatrix} \tag{53}$$

where

$$[M_{11}] = \sum_j \sum_i \int_{v_{ji}} (m_{ji}[V^{ji}][V^{ji}]^T + [\omega^j][I_{ji}][\omega^j]^T) \, dv \tag{54}$$

$$[M_{12}] = [M_{21}]^T = \sum_j \sum_i \int_{v_{ji}} m_{ji}[V^{ji}][V_s^j]^T dv \tag{55}$$

$$[M_{12}] = \sum_j \sum_i \int_{v_{ji}} m_{ji}\{[V^{ji}]([V_c^{ji}]^T + [V_s^j]^T[Q]) + \omega^j[I_{ji}][\omega^{ji}]^T\} dv \tag{56}$$

$$[M_{22}] = \sum_j \sum_i \int_{v_{ji}} m_{ji}[V_s^j][V_s^j]^T dv \tag{57}$$

$$[M_{23}] = \sum_j \sum_i \int_{v_{ji}} m_{ji}[V_s^j]([V_e^{ji}]^T + [V_s^j]^T[Q]) \, dv \tag{58}$$

$$[M_{31}] = \sum_j \sum_i \int_{v_{ji}} (m_{ji}[V_e^{ji}][V_e^{ji}]^T + [\omega^{ji}][I_{ji}][\omega^j]^T) \, dv \tag{59}$$

$$[M_{32}] = \sum_j \sum_i \int_{v_{ji}} m_{ji}[V_e^{ji}][V_s^j]^T dv \tag{60}$$

$$[M_{33}] = \sum_j \sum_i \int_{v_{ji}} \Big(m_{ji}[V_e^{ji}]([V_e^{ji}]^T + [V_s^j]^T[Q]) + [\omega^{ji}][I_{ji}][\omega^{ji}]^T\Big) dv \tag{61}$$

In the preceding equations there are five matrices $[V^{ji}]$, $[V_s^j]$, $[V_e^{ji}]$, $[\omega^j]$, and $[\omega^{ji}]$, which we refer to as partial velocities and partial angular velocities. They play a major role in the formulation of the equations of motion, and they are at least the heart of all of the computation in the dynamic simulation of multibody systems. The superscript j refers to the body number in a multibody system (open- or closed-chain type), and i denotes the element number within body j. We should note that $[V_s^j]$ is a matrix resulting from the assumption that first the body vector $\boldsymbol{q}$ (see Fig. 2) is treated as a superficial coordinate and then ultimately is deleted at the final stage of the equations. Furthermore, we have m_{ji} and $[I_{ji}]$ which represent the mass of element i of body j and the inertia dyadic components, respectively. The integration in the equations from Eq. (54) to Eq. (61) is performed over the volume of the element. All of these arrays are found to take a special form which is explicitly given subsequently. The partial velocity array for element i of body j is given by

$$[V^{ji}] = [W] \begin{bmatrix} ([S_{q2}] + [S_{\zeta 2}])[S^{10}] \\ ([S_{q3}] + [S_{\zeta 3}])[S^{20}] \\ \vdots \\ ([S_{qj}] + [S_{\zeta j}])[S^{j-1,0}] \\ ([S_{r_{ji}}] + [S_{ji}])[S^{j0}] \\ \vdots \\ 0 \end{bmatrix} \tag{62}$$

where $[W]$ is a transformation matrix relating y and $\dot{x}$, $[S^{j0}]$ ($j = 1, 2, \ldots,$) are transformation matrices defining the direction cosine between intermediate body reference frame. $[S_{qj}]$, $[S_{\zeta j}]$, $[S_{r_{ji}}]$, and $[S_{ji}]$ are skew matrices defining the components of body vector $\boldsymbol{q}$, the translation vector ζ between bodies, the position from the local body axis frame to the center mass r, and the element shape function in the local body frame, respectively (see Fig. 2 for representation of these vectors).

The partial velocity array associated with the nodal coordinate is

$$[V_e^{ji}] = \begin{bmatrix} 0 \\ \vdots \\ 0 \\ [N]^T [S^{j0}] \\ \vdots \\ 0 \end{bmatrix} \tag{63}$$

where $[N]$ denotes the shape function matrix.

The matrix $[V_s^j]$ associated with the body vector $\bar{q}$ is composed of the transformation matrices between the bodies representing j and the fixed inertial frame $\boldsymbol{R}$

$$[V_s^j] = \begin{bmatrix} [I] \\ [S^{10}] \\ \vdots \\ [S^{j-1,0}] \\ \vdots \\ 0 \end{bmatrix} \tag{64}$$

The partial angular velocity array $[\omega^j]$ associated with the rigid body motion is given by

$$[\omega^j] = [V_s^j] \tag{65}$$

The partial angular velocity array $[\omega^{ji}]$ associated with element rotation takes the following form:

$$[\omega^{ji}] = \begin{bmatrix} 0 \\ \vdots \\ 0 \\ [\Psi]^T [S^{j0}] \\ \vdots \\ 0 \end{bmatrix} \tag{66}$$

where $[\Psi]$ is the shape function matrix representing the slope of the elements.

The moment of inertia matrix $[I_{ji}]$ in the global coordinate system is given by

$$[I_{ji}] = m_{ji} [S^{0j}] \begin{bmatrix} y^2+z^2 & -xy & -xz \\ -yx & x^2+z^2 & -yz \\ -zx & -zy & x^2+z^2 \end{bmatrix} [S^{j0}] \tag{67}$$

and m_{ji} in this case represents the mass density of element i of body j.

The matrix $[Q]$ plays an important role in deleting the coordinate $\{q\}$ which represents the distance between body joints. It has the form of an incidence matrix composed of zeros and ones, for example,

$$[Q] = \begin{bmatrix} 0 & \cdots & 1 & \cdots & 0 \\ & & & \ddots & \\ 0 & \cdots & 1 & \cdots & 0 \\ & & & \ddots & \\ 0 & & \cdots & 1 \cdots & 0 \end{bmatrix} \tag{68}$$

The generalized dynamic matrix $[C]$ is as follows:

$$[C] = \begin{bmatrix} C_{11} & C_{12} & C_{13} \\ C_{21} & C_{22} & C_{23} \\ C_{31} & C_{32} & C_{33} \end{bmatrix} \tag{69}$$

where

$$[C_{11}] = \sum_j \sum_i \int_{v_{ji}} \{ m_{ji} [V^{ji}] [\dot{V}^{ji}]^T + [\omega^j] \times ([I_{ji}] [\dot{\omega}^j]^T + [\Omega_x^{0j}] [I_{ji}] [\omega^j]^T) \} \, dv \tag{70}$$

$$[C_{12}] = \sum_j \sum_i \int_{v_{ji}} m_{ji} [V^{ji}] [\dot{V}_s^j]^T dv \tag{71}$$

$$[C_{13}] = \sum_j \sum_i \int_{v_{ji}} \{ m_{ji} [V^{ji}] ([\dot{V}_e^{ji}]^T + [\dot{V}_s^j]^T [Q]) + [\omega^j] ([I_{ji}] [\dot{\omega}^{ji}]^T + [\Omega_\rho^{0j}] [I_{ji}] [\omega^{ji}]^T) \} \, dv \tag{72}$$

$$[C_{21}] = \sum_j \sum_i \int_{v_{ji}} m_{ji} [V_s^j] [\dot{V}^{ji}]^T dv \tag{73}$$

$$[C_{22}] = \sum_j \sum_i \int_{v_{ji}} m_{ji} [V_s^j] [\dot{V}_s^j]^T dv \tag{74}$$

$$[C_{23}] = \sum_j \sum_i \int_{v_{ji}} m_{ji} [V_s^j] ([\dot{V}_e^{ji}]^T + [\dot{V}_s^j]^T [Q]) \, dv \tag{75}$$

$$[C_{31}] = \sum_j \sum_i \int_{v_{ji}} \{ m_{ji} [V_e^{ji}] [\dot{V}^{ji}]^T + [\omega^{ji}] \times ([I_{ji}] [\dot{\omega}^j]^T + [\Omega_x^{0j}] [I_{ji}] [\omega^j]^T) \} \, dv \tag{76}$$

$$[C_{32}] = \sum_j \sum_i \int_{v_{ji}} m_{ji} [V_e^{ji}] [\dot{V}_s^j]^T dv \tag{77}$$

$$[C_{33}] = \sum_j \sum_i \int_{v_{ji}} m_{ji} \{ [V_e^{ji}] ([\dot{V}_e^{ji}]^T + [\dot{V}_s^j]^T [Q]) + [\omega^{ji}] ([I_{ji}] [\dot{\omega}^{ji}]^T + [\Omega_\rho^{0j}] [I_{ji}] [\omega^{ji}]^T) \} \, dv + [C_s] \tag{78}$$

where the overdot denotes differentiation with time t; $[\Omega_x^{0j}]$ and $[\Omega_\rho^{0j}]$ are skew matrices associated with rigid body and element rotation, respectively. $[C_s]$ is the ordinary damping matrix of the bodies associated with viscoelasticity properties of the body material. The components of matrix $[C]$ make use of the partial velocities and their rate of change, and they contain all of the dynamic nonlinear terms arising from the coupling between rigid and flexible motion, Coriolis effects, quadratic velocity terms, etc.

The generalized stiffness matrix $[K]$ plays an important role in the analysis of elasto-plastic bodies expressed in terms of the modal coordinates only

$$[K] = \begin{bmatrix} 0 & & \\ & 0 & \\ & & K_{33} \end{bmatrix} \tag{79}$$

where K_{33} is the ordinary stiffness matrix when all other effects are neglected. Note that the $[K]$ premultiply $\{y\}$, therefore only the components that premultiply ρ are nonzero, which represents the contribution from the linear strain energy.

The generalized force vector $\{F\}$ is given by

$$\{F\} = \begin{bmatrix} F_1 \\ F_2 \\ F_3 \end{bmatrix} \tag{80}$$

where

$$\{F_1\} = \sum_j \sum_i \int_{s_{ji}} ([V^{ji}]\{f_{ji}\} + [\omega^j]\{M_{ji}\})\,ds + \sum_j \sum_i \int_{v_{ji}} [V^{ji}]\{b_{ji}\}\,dv \tag{81}$$

$$\{F_2\} = \sum_j \sum_i \int_{s_{ji}} [V_s^j]\{f_{ji}\}\,ds + \sum_j \sum_i \int_{v_{ji}} [V_s^j]\{b_{ji}\}\,dv \tag{82}$$

$$\{F_3\} = \sum_j \sum_i \int_{s_{ji}} ([V_e^{ji}]\{f_{ji}\} + [\omega^{ji}]\{M_{ji}\})\,ds + \sum_j \sum_i \int_{v_{ji}} [V_e^{ji}]\{b_{ji}\}\,dv \tag{83}$$

where $\{f_{ji}\}$, $\{b_{ji}\}$, and $\{M_{ji}\}$ denote external surface traction, external body force, and external surface distributed moment, respectively. In what follows we will show how the material nonlinearities, creep, and other nonlinearities contribute to the equations of motion.

The formulation of the equations of motion as just described enables us to account for all of the nonlinearities discussed in the preceding sections. For instance, in the case of high temperature, all terms in the equation of motion remain the same as those given earlier, except for the $[K_{33}]$ and $\{F_3\}$ terms, which take the following form:

$$[K_{33}] = \sum_j \sum_i \int_{v_{ji}} [B]^T [D]\,[B]\,dv \tag{84}$$

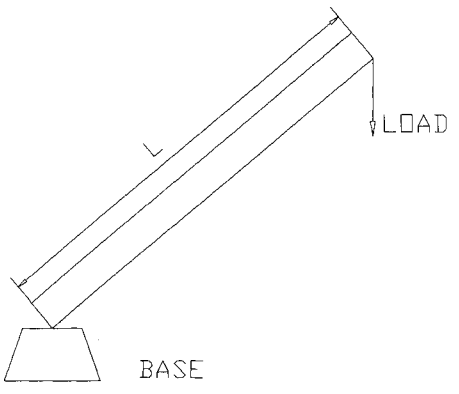

Fig. 3 Robotic manipulator.

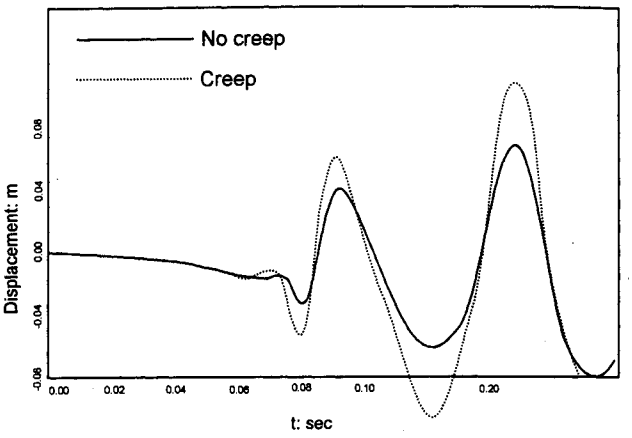

Fig. 4 Creep simulation 1.

where the material property matrix $[D]$ should be substituted by $[D_t]$ if we consider the material nonlinearities. On the other hand, if we consider the elastic-plastic deformation, $[D]$ is given by

$$[D] = [D_e] + [D_p]$$

which is defined by Eq. (35).

The $\{F_3\}$ component in the generalized force vector $\{F\}$ now becomes

$$\{F_3\} = \sum_j \sum_i \int_{s_{ji}} ([V_e^{ji}]\{f_{ji}\} + [\omega^{ji}]\{\mathfrak{M}_{ji}\})\,ds + \sum_j \sum_i \int_{v_{ji}} [V_e^{ji}]\{b_{ji}\}\,dv + \{F_T\} \tag{85}$$

where $\{F_T\}$ is the equivalent force due to creep, thermal stress, thermal shock, and temperature distribution.

$$\{F_T\} = \sum_j \sum_i \int_{v_{ji}} \left\{ [B^T][D]\,[\{\epsilon_e\} + \alpha(\{T\} + \sigma^*\{T_0\})] + \alpha[N]^T[D]\{T'\} \right\} dv \tag{86}$$

where $\{\epsilon_e\}$, α, T_0, $\{T'\}$, and σ^* are given by Eqs. (9), (14), and (15), respectively.

A flexible multibody system usually contains a great many elements, nodes, and coordinates. The problem of computing can be reduced further making use of the nodal-modal transformation matrix such that

$$\{\rho\} = [\Phi]\{\eta\} \tag{87}$$

where $[\Phi]$ denotes the modal shape matrix found through the ordinary eigenvalue problem. (Note that the transformation will yield a new representation of the equations of motion.)

IV. Numerical Simulation

Several cases of material, creep, thermoelastic, and geometric effects are presented in this paper. From these cases we have chosen to test the effects of creep on the dynamics of a robot arm. Creep in the context of large rotation has yet to be fully investigated; therefore, this simulation will help us illustrate its effects. Consider a robotic arm with a periodic time variant angular velocity undergoing large rotation. The angular velocity is selected such that the geometric stiffening effects would not be pronounced: hence, the arm deflection is mainly due to its elastic properties. Furthermore, we subject the robotic arm to creep conditions. The manifestation of creep is being sought. For the robotic arm shown

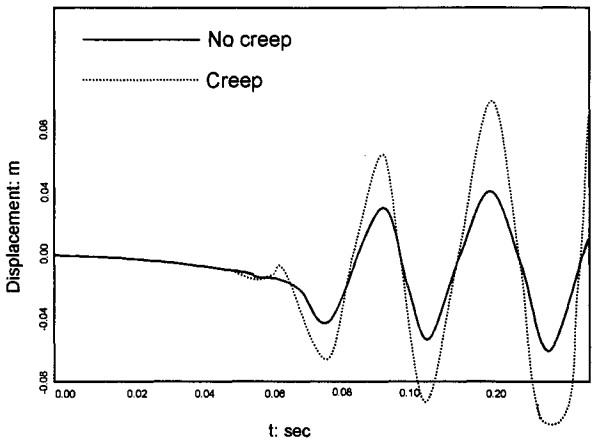

Fig. 5 Creep simulation 2.

in Fig. 3, the following data are used: the link length is $l = 1.0$ m, and its cross-sectional area is denoted by height $h = 0.1$ m and thickness $t = 0.01$ m; the Young's modulus of elasticity $Y = 2.0 \times 10^{11}$ N/m^2; Poisson ratio is assumed $\nu = 0.29$; and mass load $m_p = 10$ kg is attached to the end link. The flexible link is discretized into 20 triangular elements. Only creep is considered in the simulations. The creep strain takes Andrade's formula given by Eq. (2), where $\beta = \kappa = 1.0 \times 10^{-6}$; and the dynamic creep coefficient $k = 0.75$. Assume the angular velocity to be given by a periodic function of the form $\dot{\theta}_1 = A\omega \cos \omega t$.

In simulation 1, $A = 2.0$ rad, $\omega = 5.0$ rad/s , and the initial conditions are set equal to zero. The solid curve shown in Fig. 4 represents the deformation of the tip of link without creep, and the dashed curve represents the deformation with creep. The dynamic response for both curves is simulated for 0.2 s after time $t = 1.5 \times 10^6$ s.

In simulation 2 shown in Fig. 5, $A = 2.0$ rad, $\omega = 5.0$ rad/s , and the initial conditions are such that the velocity of each node equals zero whereas the initial displacement is equal to the static deformation due to the gravitational force.

The two simulations clearly indicate how creep manifests itself in terms of softening effects where deformation starts increasing drastically. In these simulations after 0.2 s, considering the creep effects, the tip deformation is about 0.08 m and diverging. The creep conditions damage the structure material stiffness characteristics, which in turn exponentially increase the softening effects and element inertia forces.

The effects of high temperature are very common in certain engineering applications and we anticipate that with the advent of technology, robots will be working continuously over large periods of time in these environmental conditions. Creep effects will then become very pronounced and will eventually have to be integrated into the dynamics of such systems. To this end we need to investigate the dominant effects of dynamic creep and the stage at which it needs to be controlled. We have observed how the contribution of creep affects the position and deflection of the tip of the robot arm. Since creep is closely related to the strain and strain rate of change, we can say that the deformation of a flexible body could be altered significantly under creep conditions. What needs to be investigated further are the effects of other nonlinearities in the presence of creep.

V. Conclusion

This paper presents an explicit formulation of the dynamical equations of motion for treelike systems considering the effects of general flexibility of the bodies. This includes the thermo-elastic-plastic deformation, effects of creep, thermal shock, and material and geometric nonlinearities. The equations as presented have a broad range of applications including crash simulation, space structure applications, and robotics with nuclear applications. The paper also shows how Kane's equation combined with finite element and continuum mechanics could lead to equations of motion that rely greatly on the concepts of partial velocities and partial angular velocities and their rates of change. The equations of motion in their developed form are suited for computer implementation. Their matrix representation makes them suitable to vectorization and parallel processing techniques used in real-time simulation.

References

[1]Amirouche, F. M. L., and Ider, S. K., "A Recursive Formulation of the Equations of Motion for Articulated Structures with Closed Loops—An Automated Approach," *Computers and Structures*, Vol. 30, No. 5, 1988, pp. 1135–1145.

[2]Simo, J. C., and Vu-Quoc, "On the Dynamics of Flexible Bodies under Large Overall Motions—The Plane Case: Parts I and II," *Journal of Applied Mechanics*, Vol. 53, 1986, pp. 849–863.

[3]Modi, V. J., and Likins, P. W., "On the Dynamics of Flexible Orbiting Structures," *Large Space Structures: Dynamics and Control*, edited by S. N. Atluti and A. L. Amos, Springer-Verlag, New York, 1988, pp. 93–114.

[4]Zeiler, T., and Buttrill, C., "Dynamic Analysis of an Unrestrained Rotating Structure through Nonlinear Simulation," *Proceeding of the AIAA/ASME/ASCE/AHS 27th Structures, Structural Dynamics and Materials Conference*, AIAA Washington, DC, April 1988, pp. 830–837.

[5]Banerjee, A. K., and Dickens, J. M., "Dynamics of an Arbitrary Flexible Body in Large Rotation and Translation," *Journal of Guidance, Control, and Dynamics*, Vol. 13, 1990, pp. 221–227.

[6]Kane, R. A., Ryan, R. R., and Banerjee, A. K., "Dynamics of a Cantilever Beam Attached to a Moving Base," *Journal of Guidance, Control, and Dynamics*, Vol. 10, No. 3, 1987, pp. 139–151.

[7]Amirouche, F. M. L., and Xie, M., "Dynamic Analysis of Flexible Multibody Systems with Time Variant Mode Shapes," 13th Biennial ASME Conference, Mechanical Vibration and Noise, Paper No. 34: 261-267, Miami, FL, Sept. 1991.

[8]Amirouche, F. M. L., and Xie, M., *Computational Methods in a Multibody Dynamics*, Prentice-Hall, Englewood Cliffs, NJ, 1992.

[9]Xie, M., "Dynamics of Flexible Rotorcraft System Analysis," Ph.D Dissertation, Department of Mechanical Engineering, Univ. of Illinois, Chicago, IL, March 1992.

[10]Bathe, K. J., "Finite Element Formulations for Large Deformation Dynamic Analysis," *International Journal for Numerical Method in Engineering*, Vol. 9, 1975, pp. 353–386.

[11]Hibbit, H. D., "Finite Element Formulation for Problems of Large Strain and Large Displacement," *International Journal of Solids and Structures*, Vol. 6, 1970, pp. 1069–1086.

[12]Heifitz, J. H., and Costantino, J. J., "Dynamic Response of Nonlinear Media at Large Strains," *Journal of Engineering Mechanics*, Vol. 98, 1972, pp. 1511–1527.

[13]Bathe, K. J., and Bolourchi, S., "Large Displacement Analysis of Three-Dimensional Beam Structures," *International Journal of Numerical Method in Engineering*, Vol. 14, 1979, pp. 961–986.

[14]Rabotnov, R. N., *Creep Problem in Structural Members*, John Wiley, New York, 1969.

[15]Andrade, C., *Creep and Recovery*, American Society for Metals, Park, OH, 1957, pp. 176–198.

[16]Garofalo, F., *Properties of Crystalline Solids*, ASTM Spec. Tech. Publ., Vol. 283, 1960, p. 82.

[17]Kraus, H., *Creep Analysis*, Wiley, New York, 1980.

[18]Gittus, J., *Creep, Viscoelasticity and Creep Fracture in Solids*, Wiley, New York, 1975.

[19]Chen, W. F., and Han, D. H., *Plasticity for Structural Engineering*, Springer-Verlag, New York, 1988.

[20]Boyle, J. T., and Spence, J., *Stress Analysis for Creep*, Butterworth, Boston, MA, 1983.

[21]Ohtani, R., *High Temperature Creep-Fatigue*, Elsevier Applied Science, Japan, 1988.

[22]Manson, S. S., *Thermal Stress and Low-Cycle Fatigue*, McGraw-Hill, New York, 1966.

[23]Zienkiewcz, O. C., *The Finite Element Method*, McGraw-Hill, London, 1977.

[24]Harris, B., *Engineering Composite Materials*, Print Power, London, 1986.

[25]Herrman, G. (ed.), *Dynamics of Structural Solids*, ASME, New York, 1968.

[26]Garg, S. K., *Analysis of Structural Composite Materials*, Marcel Dekker, New York, 1973.

[27]Tsai, S., "Structural Behavior of Composite Materials," NASA Rept. CR71, July 1964.

[28]Miller, A. K. (ed.), *Unified Constitutive Equations for Creep and Plasticity*, Elsevier Applied Science, New York, 1987.

[29]Ider, S. K., and Amirouche, F. M. L., "Influence of Geometric Nonlinearities in the Dynamics of Flexible Tree-like Structures," *Journal of Guidance, Control, and Dynamics*, Vol. 12, 1989, pp. 830–837.